

Evidence for a Michaelis–Menten Type Mechanism in the Electrocatalytic Oxidation of Mercaptopropionic Acid by an *Amavadine* Model

M. Fátima C. Guedes da Silva,[†] J. Armando L. da Silva,[†]
João J. R. Fraústo da Silva,^{*,†} Armando J. L. Pombeiro,^{*,†}
Christian Amatore,^{*,‡} and Jean-Noël Verpeaux[‡]

Contribution from the Complexo I, Instituto Superior Técnico, Av. Rovisco Pais, 1096 Lisboa Codex, Portugal, and Ecole Normale Supérieure, Département de Chimie, URA CNRS 1679, 24 rue Lhomond, F-75231 Paris Cedex 05, France

Received March 4, 1996. Revised Manuscript Received June 4, 1996[⊗]

Abstract: The *amavadine* complex and its model $[VL_2]^{2-}$ ($L = ^-ON[CH(CH_3)COO^-]_2$ (HIDPA³⁻) or $^-ON(CH_2COO^-)_2$ (HIDA³⁻), respectively) undergo, in aqueous medium and at a Pt electrode, a fully electrochemical and chemical reversible $V^{IV/V}$ oxidation and act as electron-transfer mediators in the electrocatalytic oxidation of some thiols (HSR) such as $HS(CH_2)_nCOOH$ ($n = 1$ or 2 , *i.e.*, mercaptoacetic or mercaptopropionic acid, respectively) and $HSCH_2CH(NH_2)COOH$ (cysteine) to the corresponding disulfides (RS-SR) which were isolated upon bulk preparative electrolyses. As shown by digital simulation of cyclic voltammetry, this redox catalysis process occurs through an unprecedented mechanism involving Michaelis–Menten type kinetics with formation ($k_1 = 1.2 \times 10^3 M^{-1} s^{-1}$) of an intermediate species (with half-life time of *ca.* 0.3 s) derived from the interaction of the oxidized vanadium complex (the active form of the mediator) with the substrate. A possible biological role for *amavadine* is suggested by these results.

Introduction

The importance of vanadium in Biology is a matter of current and growing interest, and the natural occurrence of this metal has already been recognized in a few cases, in particular in the cofactor of an alternative nitrogenase in some azotobacteria (*e.g.*, *A. vinelandii* and *A. chroococcum*), in haloperoxidases present in some algae, lichen, and terrestrial fungi (*e.g.*, *Filariopsis brevipes*, *Ascophyllum nodosum*, etc.), in some ascideans (tunicates) (*e.g.*, *Ascidia nigra*, *Phallusia mammillata*, etc.) and fan-worms (*Pseudopotamilla ocellata*), and in some *Amanita* toadstools (*A. muscaria*, *A. regalis*, and *A. velatipes*).^{1–4}

A natural vanadium (IV) complex called *amavadine* could be isolated from *Amanita* mushrooms.⁷ Firstly described as an oxovanadium (IV) species,⁷ this compound has then been shown to display a remarkable octacoordinated V^{4+} center with two tribasic HIDPA³⁻ ligands (tribasic form of 2,2'-(hydroxiimino)-dipropionic acid $HON\{CH(CH_3)CO_2H\}$).^{5,6} Even if the biological function of *amavadine* has not yet been fully elucidated, it has been assumed to play a significant role in the specific oxidation of some thiols into disulfides. This could namely happen in the protective/defensive system of the mushrooms⁸

where the disulfide bridges would bring about the cross-linking of protein fibers necessary for the regeneration of damaged tissues.

Organic thiols or thiolates can be oxidized to disulfides by simple electron uptake, by means of outersphere oxidants or at the electrode.⁹ In this respect, *amavadine* with its stable octacoordinated structure could very well belong to the class of transition metal centered natural compounds acting as pure electron donors or acceptors, in the same way as blue copper proteins, cytochromes, or iron sulfur clusters. This hypothesis is even reinforced by the fully reversible cyclic voltammogram obtained upon oxidation of *amavadine*^{10a} and the spectroscopic data of this compound and its oxidation product,⁶ all studies leading to an identical geometrical structure for both vanadium (IV) and (V) derivatives.

In the search of better analytical methods for thiols, Riechel *et al.* showed that *amavadine* can indeed act as a redox mediator for the oxidation of natural thiols such as glutathione or cysteine.^{10b} Although not orientated toward mechanistical goals, some of the data therein suggested that a nonclassical redox catalysis mechanism was operative. This looked rather surprising with regards to the expected outersphere oxidation mechanism.⁶ We therefore decided to investigate thoroughly the mechanism of *amavadine* mediated oxidation of biological thiols in aqueous medium in order to bring evidence for a specific interaction between the substrate and the oxidized form of the mediator rather than a simple outersphere electron transfer. The

(7) Bayer, E.; Kneifel, H. *Z. Naturforsch.* **1972**, *27B*, 207. Kneifel, H.; Bayer, E. *Angew. Chem., Int. Ed. Engl.* **1973**, *12*, 508.

(8) Fraústo da Silva, J. J. R. *Chem. Speciation Bioavailability* **1989**, *1*, 139. A similar function for vanadium in tunicates has also been proposed, although the metal is in a lower oxidation state, see: Smith, K. J. *Experientia* **1989**, *45*, 452, and references therein.

(9) Svensmark, B.; Hammerich, O. In *Organic electrochemistry. An introduction and a guide*, 3rd ed.; Lund, H., Baizer, M. M., Eds.; Chapter 17. Oxidation of sulfur containing compounds; Marcel Dekker: New York, 1991; p 659.

(10) (a) Nawi, M. A.; Riechel, T. L. *Inorg. Chim Acta* **1987**, *136*, 33. (b) Thackerey, R. D.; Riechel, T. L. *J. Electroanal. Chem.* **1988**, *245*, 131.

[†] Instituto Superior Técnico.

[‡] Ecole Normale Supérieure.

[⊗] Abstract published in *Advance ACS Abstracts*, July 15, 1996.

(1) Fraústo da Silva, J. J. R.; Williams, R. P. *The Biological Chemistry of the Elements. The Inorganic Chemistry of Life*; Clarendon Press: Oxford, 1993.

(2) Metal ions in Biological systems; Siegel, H., Siegel, A., Eds.; Marcel Dekker, Inc.: 1995; Vol. 31.

(3) Fraústo da Silva, J. J. R. *et al.*, work in progress.

(4) Vollenbroek, E. G. M.; Simons, L. H.; van Schijndel, J. W. P. M.; Barnett, P.; Bolzar, M.; Dekker, H.; van der Linden, C.; Weber, R. *Plant Peroxidases, Struct. Mol. Biol.* **1995**, *23*, 267.

(5) Carrondo, M. A. F. de C. T.; Duarte, M. T. L. S.; Pessoa, J. C.; Silva, J. A. L.; Fraústo da Silva, J. J. R.; Vaz, M. C. T. A.; Vilas-Boas, L. F. *J. Chem. Soc., Chem Commun.* **1988**, 1158.

(6) Armstrong, E. M.; Beddoes, R. L.; Calviou, L. J.; Charnock, J. M.; Collison, D.; Ertok, N.; Naismith, J. H.; Garner, C. D. *J. Am. Chem. Soc.* **1993**, *115*, 807.

results described in this work show that a Michaelis–Menten type mechanism involving the interaction of the substrate with the oxidized form of the mediator actually takes place. It is established that such a mechanism, frequently invoked to interpret the enzymatic activity,¹¹ can also operate in electrocatalytic processes, a result with evident significance in biology.

Results

Electrochemical Behavior of the Amavadin Complex and Its Model. The electrochemical behavior of the complexes $[\text{VL}_2]^{2-}$ ($\text{L} = \text{hidpa}^{3-}$ or HIDA^{3-}) was studied by cyclic voltammetry and controlled potential electrolysis, in 0.1 M KCl aqueous solutions and at a platinum-disc ($\phi = 0.5$ mm) or -gauze working electrode, respectively. The complexes undergo a single-electron reversible oxidation (at $E^\circ = 0.49$ or 0.52 V vs SCE, respectively) corresponding to the $\text{V}^{\text{IV}} \rightleftharpoons \text{V}^{\text{V}}$ interconversion (Figure 1). In agreement, the heterogeneous electron transfers are fast, as indicated by peak-to-peak separation ($\Delta E_p = E_{\text{pa}} - E_{\text{pc}}$) and half-width ($\Delta E_{p/2} = E_{\text{pa}} - E_{p/2a}$) values (70 ± 5 mV and 55 ± 5 mV, respectively, determined at a scan rate of 0.2 V s^{-1}) which are identical to those obtained for $\text{K}_4\text{[Fe(CN)}_6\text{]}$ under the same experimental conditions. Moreover, controlled potential electrolysis at a potential slightly higher than E_{pa} consumes 1 Faraday/mol to afford the V^{V} species, which is unstable and consequently difficult to isolate since it slowly reverts to the parent V^{IV} presumably by oxidation of water. In the scan rate range under study, $0.05\text{--}20$ V s^{-1} , the current function is constant.

Electrochemical Behavior of $[\text{V}(\text{HIDA})_2]^{2-}$ in the Presence of Mercaptopropionic Acid. The $[\text{VL}_2]^{2-}$ systems of this study are involved in the electrocatalytic oxidation of thiols such as mercaptoacetic and mercaptopropionic acids [HSCH_2COOH and $\text{HS}(\text{CH}_2)_2\text{COOH}$, respectively] as well as, for example, cysteine [$\text{HSCH}_2\text{CH}(\text{NH}_2)\text{COOH}$], in unbuffered solutions.¹² It was also observed that the electrocatalytic effect is completely lost by replacement of the thiol group by an hydroxyl or an alkylthioether moiety or of the apparently necessary activating carboxylic group by an amine, a methyl, a methylenethiol, a sulfonate, or an hydroxide. In fact, no catalytic effect was detected for serine [$\text{HOCH}_2\text{CH}(\text{NH}_2)\text{COOH}$], methionine [$\text{CH}_3\text{S}(\text{CH}_2)_2\text{CH}(\text{NH}_2)\text{COOH}$], 2-aminoethanethiol ($\text{HSCH}_2\text{CH}_2\text{NH}_2$), propanethiol ($\text{HSCH}_2\text{CH}_2\text{CH}_3$), 1,3-propanedithiol ($\text{HSCH}_2\text{CH}_2\text{CH}_2\text{SH}$), 2-mercaptoethanesulfonic acid, sodium salt ($\text{HSCH}_2\text{CH}_2\text{SO}_3\text{Na}$) (coenzyme M), or 2-mercaptoethanol ($\text{HSCH}_2\text{CH}_2\text{OH}$).¹⁴

As shown in Figure 1, the catalytic nature of the anodic waves is evident from the enhancement of the anodic peak current upon

(11) Bailey, J. E.; Ollis, D. F. *Biochemical Engineering Fundamentals*, 2nd ed.; MacGraw-Hill Book Company: New York, 1986.

(12) No pH effect on the electrochemical behavior of the vanadium system was detected under our experimental conditions, either by using the previously prepared complexes $[\text{VL}_2](\text{H}_3\text{O})_2$ ($\text{L} = \text{HIDA}^{3-}$ or HIDPA^{3-}), see Experimental Section, pH ca. 5, or when generating *in situ* the $[\text{VL}_2]^{2-}$ species (pH ca. 2). This can be accounted for in terms of the following arguments: (i) the stability constants of the *amavadin* complex $[\text{V}(\text{HIDPA})_2]^{2-}$ and its model $[\text{V}(\text{HIDA})_2]^{2-}$ are so high (greater than 10^{21} , see ref 13a) that they remain practically undissociated at quite low pH values (even lower than those observed in our systems); (ii) for pH values (as those of our experiments and in biological medium) well below the pK_a value of the functional thiol group of our substrates (e.g., 10.8 for mercaptoacetic acid, see ref 13b), these are practically all in the acid ($-\text{SH}$) form; (iii) the form of the carboxylic functional groups of our substrates should not play a relevant role in view of the recognized (see also ref 10b) activity for thiols with either a carboxylic or an ester group.

(13) (a) Anderegg, G.; Koch, E.; Bayer, E. *Inorg. Chim. Acta* **1987**, *127*, 183. (b) Smith, R. M.; Martell, A. E. *Critical Stability Constants*; Plenum Press: New York, 1977; Vol. 3.

(14) Fraústo da Silva, J. J. R.; Guedes da Silva, M. F. C.; da Silva, J. A. L.; Pombeiro, A. J. L. *Molecular Electrochemistry of Inorganic, Bioinorganic and Organometallic Compounds*; Kluwer Academic Publishers: The Netherlands, 1993; p 411.

$i \times 10^5 / \text{A}$

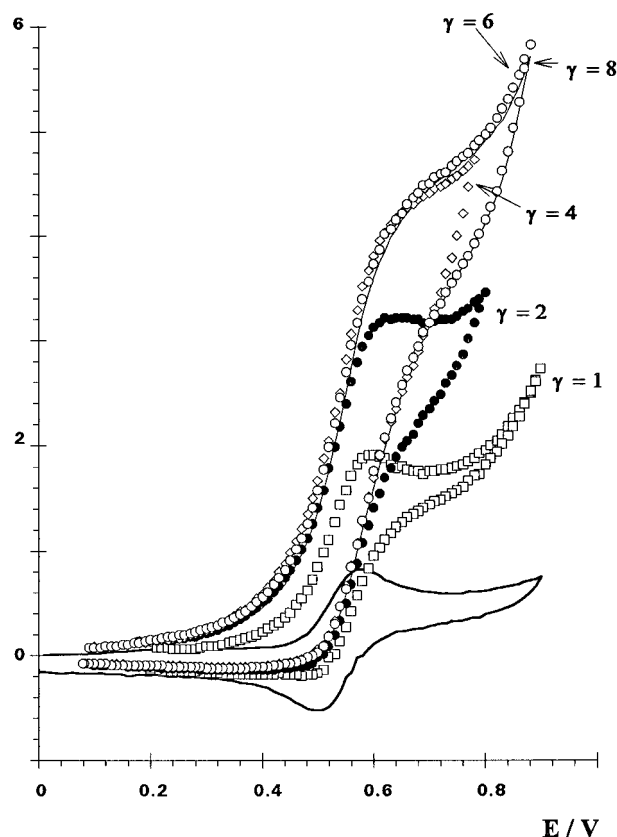


Figure 1. Cyclic voltammograms for the $[\text{V}(\text{HIDA})_2]^{2-}$ complex (solid line) and for the vanadium complex/ $\text{HS}(\text{CH}_2)_2\text{COOH}$ system (symbols) in 0.2 M KCl/ H_2O , at a platinum disc working electrode ($\phi = 0.5$ mm) and at a scan rate of $\nu = 0.2$ V s^{-1} . The γ values indicate the ratio between the thiol and the vanadium complex concentrations.

the addition of increasing amounts of mercaptopropionic acid (as indicated by the different values of the excess factor γ , defined as the ratio between the substrate and the electron mediator concentrations $[\text{S}]/[\text{M}]$) for which, in the absence of the vanadium system, no direct anodic oxidation has been detected. However, a simple EC catalytic mechanism^{15,16} was in contradiction with the dramatic suppression effect on the catalytic activity of the mediator (Figure 1) by a relatively high thiol concentration. This is evident from the plot of $(i_c - i_o)/i_o$ vs $[\text{S}]$ at different scan rates (Figure 2). It is also noteworthy that the different plots (Figure 3) of i_c/i_o vs $-\log(\nu)$ establish that there is no saturation effect with the scan rate since $(i_c - i_o)/i_o$ increases upon decreasing the scan rate even in the range where the saturation effect with the substrate concentration is observed.

The possibility of coordination of the thiol to any of the redox forms of the vanadium complex was also taken into account. However, the cyclic voltammetric investigation at high scan rates ($\nu > 5$ V s^{-1} , i.e., when a completely chemically reversible wave is observed for the $\text{V}^{\text{IV}}/\text{V}^{\text{V}}$ couple) indicated that the E° of the $\text{V}^{\text{IV}}/\text{V}^{\text{V}}$ redox pair was not affected by the presence of the thiol ($\gamma \leq 8$) as apparent by an identical value for the E° and for the peak-to-peak separation.

Preparative scale electrolysis was performed in the presence of 8 equiv of the thiol (HSR) leading to a consumption of 9

(15) Andrieux, C. P.; Dumas-Bouchiat, J. M.; Savéant, J. M. J. *Electroanal. Chem.* **1980**, *113*, 1.

(16) Bard, A. J.; Faulkner, L. R. *Electrochemical Methods. Fundamentals and Applications*; John Wiley & Sons: New York, 1980; p 438, Table II.2.1, case 6.

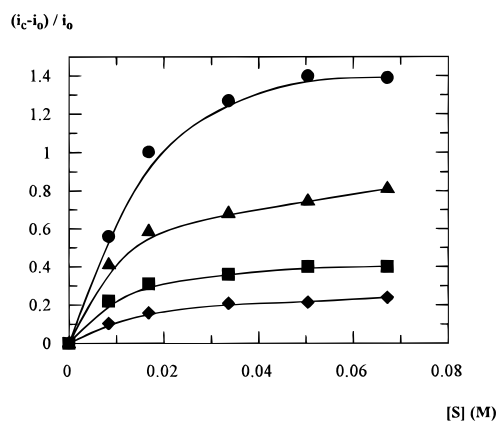


Figure 2. Plot of the normalized peak current $(i_c - i_0)/i_0$ vs the substrate concentration $[S]$, for the $[V(HIDA)_2]^{2-}/HS(CH_2)_2COOH$ system. Scan rate of 0.05 (●), 0.1 (▲), 0.2 (■), and 0.4 (◆) $V s^{-1}$. $[S]$ in M. Concentration of the HIDA complex, $c = 8.4$ mM.

Faraday/mol of vanadium complex. The final product, with low solubility in the aqueous electrolyte solution, was isolated by filtration and characterized by the usual techniques of elemental microanalysis and IR spectroscopy. A comparison of the obtained results with those of an authentic sample identified the product as the dimer RS-SR (ca. 85% isolated average yield).

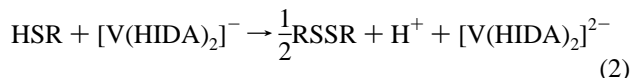
The electrochemistry of the *amavadine* and its model in the presence of other thiols (cysteine and mercaptoacetic acid) essentially showed identical results, with the V^V species mediating their oxidation in a process involving a saturation with the substrate concentration and not with the lowering of the potential scan rate. Moreover, preparative scale electrolysis of each thiol in the presence of the vanadium complex ($\gamma = 12$ for cysteine, $\gamma = 8$ for mercaptoacetic acid) yielded the corresponding disulfides with the consumption of 1 e^- /molecule of thiol in addition to 1 e^- /molecule of the vanadium complex.

Discussion

The complexes $[V(HIDA)_2]^{2-}$ and $[V(HIDPA)_2]^{2-}$ undergo a fully electrochemical and chemical reversible V^{IV}/V^V oxidation process (eq 1 for the former species) in the range of scan rates under study (0.05–20 $V s^{-1}$).



In the presence of the investigated thiols HSR (mercaptopropionic acid, mercaptoacetic acid and cysteine), the oxidized vanadium species is able to promote their oxidation converting them into the corresponding disulfide derivatives (eq 2).



Under preparative and transient electrochemical experiments, combination of the processes in eqs 1 and 2 yields to mediated oxidation of the thiols at the oxidation potential of the V^{IV} complex. This agrees with observations reported by others¹⁰ for the behavior of some biological thiols (glutathione, cysteine, cysteine methyl ester, or penicillamine) in the presence of the *amavadine* complex, at a glassy carbon electrode, although the mechanism was then not investigated. We now report the results of the detailed mechanistic study we have performed on the abovementioned electrocatalytic processes.

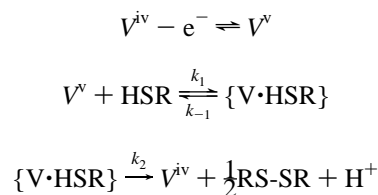
Our cyclic voltammetric investigation showed that despite the facile mediated electro-oxidation of the thiols, the overall process did not behave as expected for a classical redox catalytic

process.^{15,16} Indeed, a saturation of the redox catalyst upon increasing the substrate concentration is observed. Moreover, this saturation effect with the thiol concentration is not associated to a similar saturation upon decreasing the scan rate. This indicates that the process at hand cannot be described in terms of a classical redox catalysis mechanism¹⁷ which implies no saturation effect with the scan rate or substrate concentration provided that the substrate is in excess. It does not fit either to a complicated redox catalysis involving a progressive quenching of the mediator by formation of a stable product with the activated substrate.¹⁸ This would imply a saturation of the redox catalytic effect with both the scan rate and the concentration. Moreover, and in contrast with the latter mechanism, product analysis of the electrolysed solution of the thiol in the presence of the vanadium complex yielded no indication of the formation of a stable adduct between the mediator and the substrate.

We are then forced to conclude that the vanadium mediated oxidation of thiols proceeds along a mechanism that differs significantly from the redox catalysis mechanisms that have been considered and investigated up to now.^{15–18}

The detection of a saturation of the catalytic efficiency with the substrate concentration associated with no saturation upon increasing the time scale of the experiment (*i.e.*, decreasing the scan rate) is very reminiscent of the classical Michaelis–Menten enzymatic kinetics.¹¹ These observations suggest that the oxidation of the thiol by the oxidized vanadium species proceeds *via* the transient formation of an adduct between the V^V species and the thiol (see Scheme 1 where V stands for $[VL_2]^{2-}$ with $L = HIDA^{3-}$ or $HIDPA^{3-}$).

Scheme 1



Indeed, the mechanism in Scheme 1 is qualitatively expected to give rise to all effects that have been observed experimentally. Thus, when the thiol is not in large excess, the regeneration of the V^{IV} species is kinetically controlled by the slow reaction of the V^V complex with the thiol leading to the observation of a classical kinetic behavior for redox catalysis.¹⁶ Increasing the thiol concentration will result in a progressive shift of the kinetic control of the regeneration process to the decomposition of the transient adduct. Then the redox catalysis overall rate becomes independent of the substrate concentration but remains dependent on the scan rate. Note that this occurs only when $k_{-1} \ll k_2$ and $k_1[HSR]$, since otherwise the formation of $\{V \cdot HSR\}$ would be equilibrated and no saturation with the substrate would be observed (*vide infra*).

Cyclic voltammetric simulation, by explicit finite differences, was used to validate quantitatively the process given in Scheme 1. The corresponding results are presented for mercaptopropionic acid as solid curves in Figure 3. The best fit was obtained for $k_1 = 1.2 \times 10^3 M^{-1} s^{-1}$, $k_2 = 2.5 s^{-1}$, and $k_{-1} \ll k_2$, and this yielded to an excellent agreement with the experimental data at several concentrations of substrate, all over the range of scan rates investigated. These results are also presented in Figure 4 under a form reminiscent of a classical Lineweaver–Burk plot¹¹ used in the treatment of homogeneous Michaelis–

(17) Andrieux, C. P.; Blocman, C.; Dumas-Bouchiat, J. M.; Savéant, J. *M. J. Am. Chem. Soc.* **1979**, *101*, 3431.

(18) Pedersen, S. U. *Acta Chim. Scand.* **1987**, *A 41*, 391.

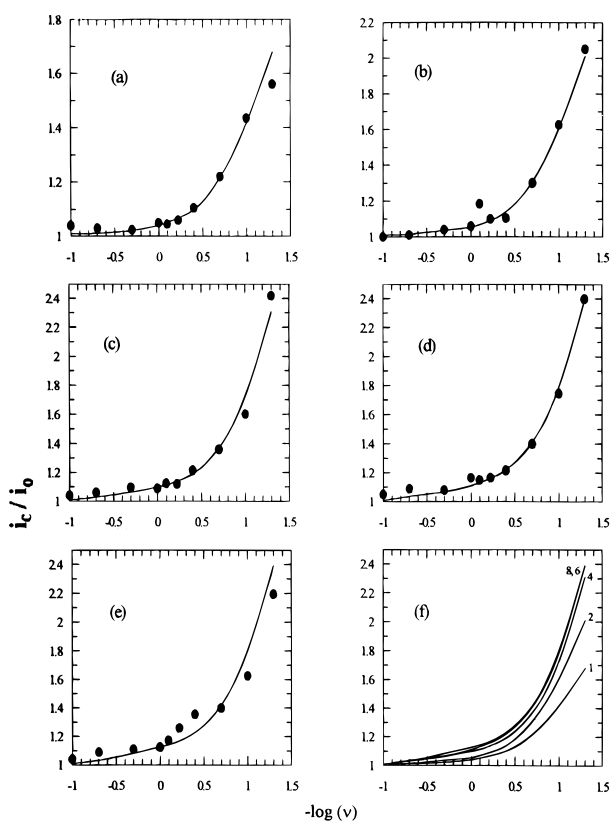
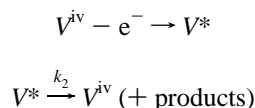


Figure 3. Plots of experimental (symbols) and simulated (lines) i_c/i_0 vs $-\log(v)$, for excess factor of 1 (a), 2 (b), 4 (c), 6 (d), 8 (e), (v in $V s^{-1}$), and (f) superimposition of the simulated curves in (a–e).

Menten enzymatic kinetics. Despite the fact that, in electrochemical experiments, reaction kinetics occur in nonhomogeneous conditions (because of the development of concentration profiles as a function of the distance from the electrode surface), it is observed that almost linear plots are obtained when $1/[(i_c/i_0) - 1]$ is plotted as a function of $1/[S]$. As shown in Figure 4, the experimental values fit reasonably well (within the experimental error)¹⁹ with the theoretical plot (solid line) obtained *via* simulation.

Of interest in the classical Lineweaver–Burk plot is the intercept and the slope of the regression line that give access, respectively, to k_2 and k_1 .¹¹ In the present case, due to the electrochemical character of the method used here, the relationship between the intercept and slope of the regression lines (shown in Figure 4) and k_1 or k_2 is less straightforward. The intercept corresponds to a kinetic situation in which all the V^V mediator is trapped instantaneously to afford the complex $\{V \cdot HSR\}$ because $k_1[HSR](RT/Fv) \rightarrow \infty$. In this case, the kinetic sequence in Scheme 1 is kinetically equivalent to the simplified sequence in Scheme 2 where V^* represents the sum of the V^V and $\{V \cdot HSR\}$ species.

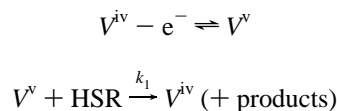
Scheme 2



Scheme 2 is equivalent to the classical catalytic $E_r C_i$ process.¹⁶ The current ratio i_c/i_0 is then only a function of $k_2 RT/Fv$. This is what is observed in Figure 5a, where the solid line represents the theoretical variation for $k_2 = 2.5 s^{-1}$. The relationship between the slope and k_1 or k_2 is less obvious. Indeed, at low concentrations of the substrate, the rate determining step of the

sequence in Scheme 1 is the complexation of the oxidized vanadium species by the thiol substrate, since $k_1[HSR] \ll k_2$. Then, the concentration of the intermediate complex $\{V \cdot HSR\}$ obeys the steady-state approximation and the sequence in Scheme 1 becomes kinetically equivalent to the simplified one in Scheme 3.

Scheme 3



This latter sequence is also equivalent to a classical redox catalysis mechanism and the kinetics depend only on $k_1[HSR]$ (RT/Fv). The dependence of i_c/i_0 on the scan rate and the thiol concentration could then be determined from previously reported works.^{20,21} However, based on the values of k_1 ($1.2 \times 10^3 M^{-1} s^{-1}$) and k_2 ($2.5 s^{-1}$) this would require (see above) a concentration of the thiol much less than the Michaelis constant $K_m = k_2/k_1 = 2.1$ mM, that is, outside the range of concentration that could be investigated by our method. Therefore, our data in Figure 4 correspond to an intermediate kinetic behavior between the two limiting cases usually considered in Michaelis–Menten kinetics. The slope could, however, be evaluated by means of a simulation procedure, and its variation with the scan rate is shown in Figure 5b. Again, a reasonable fit is obtained between the experimental data and the theoretical prediction.

In Scheme 1, a disulfide is produced. Although the mechanism of the S–S bond formation could not be investigated in the present study, our results show that the formation of the disulfide from the $\{V \cdot HSR\}$ species obeys a rate determining step that is first order in $\{V \cdot HSR\}$ and zero order in thiol, and in the vanadium V^V or V^{iv} species. Thus the disulfide formation could occur by the intermediate production of $\cdot SR$ radicals followed by fast coupling.⁹ Alternatively, one could also conceive that the intermediate species $\{V \cdot HSR\}$ undergoes some kind of reorganization (with the rate constant k_2) followed by rapid reaction with another thiol and elimination of the disulfide.

It must be stressed that only thiols with carboxylate (or ester) groups exhibit the behavior described in the present work. The presence of “activating” carbonyl seems therefore to be a prerequisite for the electrochemical oxidation of thiols mediated by *amavadin*.

Conclusions

The results obtained in this work indicate that the electrocatalytic oxidation of some thiols in the presence of *amavadin* (or a related V^{iv} complex) occurs through a novel type of redox catalysis mechanism characterized by a saturation effect with

(19) It is noteworthy that, due to its reciprocal nature, the Lineweaver–Burk kind of plot presents an experimental validity only when i_c/i_0 differs significantly from unity as evidenced by the large error bars in Figure 4 for $1/[(i_c - i_0) - 1] > 5$, i.e., $1 \leq i_c/i_0 \leq 1.2$, since our estimated accuracy is $\pm 3\%$ on i_c/i_0 . For this reason Figure 4 is presented as two different panels: (a) presents the raw results, and (b) only these which bear kinetic sense based on the experimental error.

(20) Andrieux, C. P.; Blocman, C.; Dumas-Bouchiat, J. M.; M'Halla, F.; Savéant, J. M. *J. Electroanal. Chem.* **1980**, *113*, 19.

(21) Note that the general sequence in Scheme 1 leads to another limiting case that we do not consider here because its predictions disagree with the experimental observations. This third limiting case corresponds to a situation where $k_2 \ll k_{-1}$. Then, when $k_{-1}RT/Fv \gg 1$ and $k_1 RT/Fv \gg 1$, $\{V \cdot HSR\}$ is in rapid equilibrium with V^V and HSR, this equilibrium being pulled continuously to its right-hand side (*viz.*, to the formation of V^{iv} and $1/2$ -RSSR) by the continuous evolution of $\{V \cdot HSR\}$. Thus the system is controlled by the parameter $(k_1[HSR]/k_{-1})k_2 RT/Fv$. This predicts therefore a variation of the catalytic activity similar to that in Scheme 3, *viz.*, that could be determined from literature.²⁰

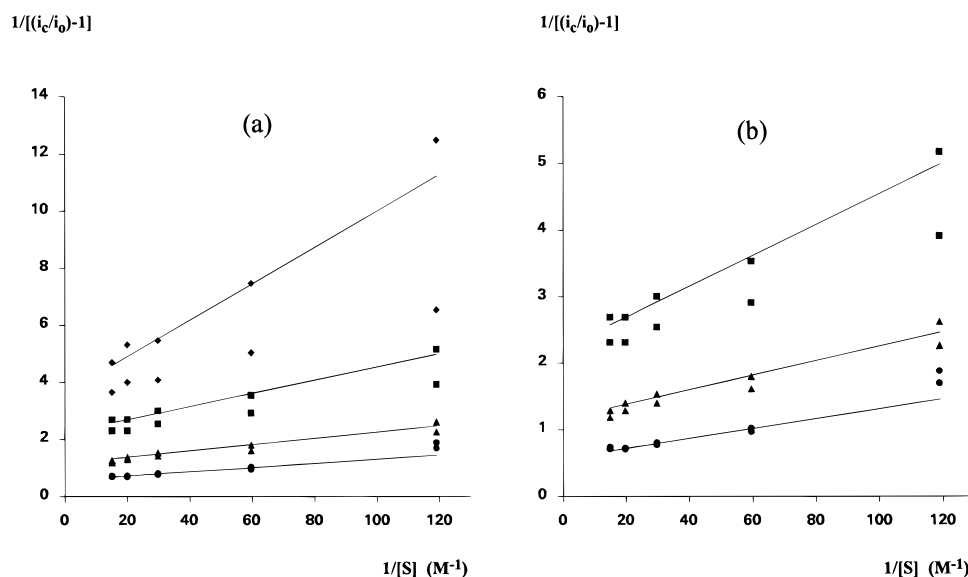


Figure 4. Plot of experimental (symbols) and simulated (lines) $1/[(i_c/i_0) - 1]$ vs $1/[S]$ for the $[V(\text{HIDA})_2]^{2-}/\text{HS}(\text{CH}_2)_2\text{COOH}$ system. Scan rate of 0.05 (●), 0.1 (▲), 0.2 (■), and 0.4 (◆) V s^{-1} . $[S]$ in M.

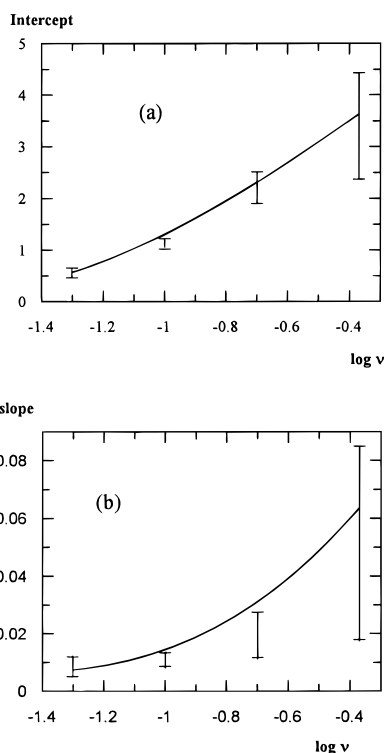


Figure 5. (a) Plot of the experimental (bars) and simulated (line) intercept of $1/[(i_c/i_0) - 1]$ vs $1/[S]$ (see Figure 4), as a function of $\log(\nu)$. $[S]$ in M, ν in V s^{-1} . (b) Plot of the experimental (bars) and simulated (line) slope of $1/[(i_c/i_0) - 1]$ vs $1/[S]$ (see Figure 4), as a function of $\log(\nu)$. $[S]$ in M, ν in V s^{-1} .

the concentration of the substrate. The kinetic analysis established that the electrogenerated active form of *amavadin* acts as an innersphere oxidant forming a complex with the thiol, the half-life time of this intermediate being in the 0.3 s range. The occurrence of this Michaelis–Menten process is of biological significance: the limitation of the efficiency of the redox catalysis due to the saturation effect is compensated by the specificity of the process associated with the recognition of the substrate. Indeed, special conditions have to be fulfilled for the oxidation of a given thiol to proceed: the necessary presence of a second functional group such as a carboxylic derivative two or three bonds away from the sulfhydryl group may suggest

a coordination to the metal due to the geometrical analogy with the initial HIDPA ligand.

Experimental Section

General Considerations. The electrochemical experiments were carried out on an EG&G PAR 173 potentiostat/galvanostat and an EG&G PARC 175 Universal programmer or on an EG&G PAR 273 potentiostat/galvanostat connected to a 386-SX personal computer through a GPIB interface. Cyclic voltammetry was undertaken in a two-compartment three electrode cell, at a Pt disc working electrode ($\phi = 0.5$ mm), probed by a Luggin capillary connected to a SCE reference electrode, on deionized water containing 0.1 M potassium chloride as supporting electrolyte. Controlled-potential electrolysis was carried out in a three electrode H-type cell with platinum gauze working and counter electrodes in compartments separated by a glass frit; a Luggin capillary, probing the working electrode, was connected to a silver-wire pseudoreference electrode. The electrochemical studies were performed in an inert atmosphere (N_2).

The mechanism of the electrocatalytic process was investigated by simulation (program CVSIM²²) of the voltammograms at different scan rates and various concentrations of reagents.

Infrared spectra were run with a Perkin Elmer 683 spectrophotometer.

The vanadyl sulfate, potassium chloride, and the organic substrates were commercially available; HIDPA (*L-N*-hydroxyimino-2,2'-dipropionic acid) and HIDA (*N*-hydroxyiminodiacetic acid) were prepared according to a published method.²³

Sample Preparation. The compounds $[\text{VL}_2](\text{H}_3\text{O})_2$ [$\text{L} = ^-\text{ON}(\text{CH}(\text{CH}_3)\text{COO}^-)_2$ or $^-\text{ON}(\text{CH}_2\text{COO}^-)_2$] were prepared by a modification of the procedure followed⁵ for the synthesis of the corresponding ammonium tetramethylammonium salt, $[\text{V}(\text{HIDA})_2][\text{NH}_4][\text{NMe}_4]$: vanadyl sulfate VOSO_4 was used instead of the chloride VOCl_2 , and treatment with $[\text{NMe}_4]\text{OH}$ and NH_4OH was avoided. Alternatively, they were generated *in situ* by adding (in a twofold excess) the appropriate acid, HIDPA or HIDA, respectively, to a VOSO_4 aqueous solution. The electrochemical behavior of the complexes was found to be independent of their generation process.

Preparative Scale Electrolysis of RS-SR ($\text{R} = \text{CH}_2\text{CH}_2\text{COOH}$ or CH_2COOH). A mixture of 0.020 g (0.050 mmol) of $[\text{V}(\text{HIDPA})_2](\text{H}_3\text{O})_2$ and 30.6 μL (0.35 mmol) of mercaptopropionic acid was electrochemically oxidized in 15 cm^3 of a 0.1 M $\text{KCl}/\text{H}_2\text{O}$ electrolyte solution, at 0.51 V vs SCE, until the complete conversion of the V^{IV} complex into the V^{V} analogue (consumption of 8 Faraday/mole), as

(22) Gosser, D. K., Jr.; Zhang, F. *J. Electroanal. Chem.* **1991**, *38*, 715.

(23) Kneifel, H.; Bayer, E. *J. Am. Chem. Soc.* **1986**, *108*, 3075.

shown by the cyclic voltammogram of the electrolyzed solution. The electrolyzed colorless solution was then transferred to a Schlenck tube and the solvent was slowly evaporated under vacuum until the formation of a white solid which was isolated by filtration and dried. Yield 85%. Anal. Calcd (found) for $S_2C_6O_4H_{10}^{1/2}H_2O$: C, 32.87 (32.72); H, 4.24 (4.79); S, 28.48 (29.22). IR (KBr pellet) $\nu(OH)$ and $\nu(CH_2-S)$ 3100–2550 cm^{-1} ; $\nu(C=O)$ 1685 cm^{-1} (strong); $\nu(C-S)$ 650–635 cm^{-1} (medium); $\nu(S-S)$ 535–510 cm^{-1} (weak).

A similar procedure was followed for the electrochemical synthesis of $HOOCCH_2SSCH_2COOH$ (cystine) which precipitated spontaneously

from the electrolyzed solution. Its IR spectrum was identical to that of a genuine sample of cystine.

Acknowledgment. This work has been partially supported by CNRS and MESR (France), the PRAXIS XXI (Portugal) program, and by the bilateral JNICT/CNRS Portugal–France protocol of collaboration.

JA9607042